International Journal of Automotive Technology, Vol. 11, No. 4, pp. 471−479 (2010)
DOI 10.1007/s12239−010−0058−5

1229−9138/2010/053−04

DEVELOPMENT AND ANALYSIS OF AN AIR SPRING MODEL

S. J. LEE*

Department of Mechanical Engineering, Myongji University, Gyeonggi 449-728, Korea

(Received 18 June 2009; Revised 23 October 2009)

ABSTRACT−The analytical model of an air spring can be effectively used for the design of air spring equipped vehicles to provide better ride and handling characteristics along with various functions for passenger convenience. However, establishing a general model of an air spring poses particular difficulties due to the severe nonlinearities in the stiffness and the hysteresis effects, which are hardly observed in conventional coil springs. The purpose of this study is to develop a general analytic model of an air spring – one which represents the main characteristics of stiffness and hysteresis and which can be connected to a model of pneumatic systems desigined to control air spring height. To this end, the mathematical model was established on the basis of thermodynamics with the assumptions that the thermodynamic parameters do not vary with the position inside the air spring, that the air has the ideal gas property, and that the kinetic and potential energies of the air are negligible. The analysis of the model has revealed that the stiffness is affected by the volume variation, the heat transfer, and the variation of the air mass and the effective area. However, the hysteresis is mainly affected by the heat transfer and the variation of the effective area. In particular, it was revealed that the increase of the volume due to the cross-sectional area increases the stiffness, while the increase of the volume due to the other reason decreases it. In addition, the model was used to develop the sufficient stability condition, and the stability of the model was analyzed. The paper also presents the comparison between the simulation and experimental results to validate the established model and demonstrates the potential of the model to be usefully employed for the development of the air spring and its algorithm for use in a pneumatic system.

KEY WORDS : Air spring, Analytic model, Stiffness, Hysteresis, Thermodynamic model, Stability

NOMENCLATURE

$\dot{m}_{in}$: air mass flow rate flowing into air spring
$\dot{m}_{out}$: air mass flow rate flowing out of air spring
m_{cv} : air mass inside air spring
V_{cv} : control volume of air spring
$\dot{Q}_{heat}$: heat transfer rate
A_{heat} : area of heat transfer
h_c : heat transfer coefficient
W : work performed on air spring
h_{in} : enthalpy flowing into air spring
h_{out} : enthalpy flowing out of air spring
U_{cv} : internal energy inside air spring
P_{cv} : pressure inside air spring
P_{atm} : pressure of environment
T_{cv} : temperature inside air spring
T_{in} : temperature of air flowing into the air spring
T_{env} : temperature of environment around air spring
c_v : specific heat at constant volume
c_p : specific heat at constant pressure
k : specific heat ratio
R : ideal gas constant
F_{as} : force applied to vehicle body by air spring
A_{eff} : effective area of air spring
z : vertical displacement
z_0 : magnitude of displacement sinusoid
f : frequency of displacement sinusoid
t : time
V_{cv0} : fixed volume of air spring
A_{cs} : cross-sectional area of the air spring
$z_{\max}$: maximum displacement of bottom of air spring
z_{curr} : current displacement of bottom of air spring

*Corresponding author. e-mail: visionsj@mju.ac.kr

1. INTRODUCTION

Air springs have been primarily applied to commercial vehicles and luxury passenger cars because they are costly. They have many advantages, however, compared with conventional coil springs. Air springs provide better comfort and improvement in the handling performance because they can have relatively low stiffness and enable a vehicle to maintain optimum wheel alignment. In addition, air springs can protect the body of a vehicle on rough roads and make the task of loading baggage into the trunk of a vehicle more convenient (Figure 1) because the heights of the air springs can be adjusted through supplying and exhausting the air via the pneumatic circuit connected to the air spring (Jang *et al*., 2007; Hyundai Motor Company, 2009; Kia Motor Company, 2009). Figure 2 shows an air spring and its relevant pneumatic system.

The analytic model can be usefully employed for the design of an air spring, the related pneumatic system, and the algorithm for the operation of the pneumatic system (Jang *et al*., 2007; Kim *et al*., 2001). However, it is very difficult to develop an accurate air spring model due to its severe nonlinearities, which are not found in conventional coil springs. More specifically, the stiffness of an air spring, which has a significant effect on the ride and handling characteristics of a vehicle, varies nonlinearly with the frequency of the road excitation. The hysteresis characteristics of an air spring, which provides a vehicle with the additional damping force, cannot be neglected compared with the force of the damper, and it also varies with the frequency of the road excitation (Nieto *et al*., 2008; Chang and Lu, 2008).

Some research works (Kim *et al*., 2001; Nieto *et al*., 2008; Chang and Lu, 2008; Kim and Kim, 2005; Quaglia and Sorli, 2001; Seong *et al*., 2008; Cha *et al*., 2006) have been carried out to develop an analytic model for an air spring involving these nonlinear characteristics. Kim *et al*. (2001) have developed a model of an air spring and a vehicle with a flexible body using ADAMS, which has been used to estimate the performance of a vehicle with a control algorithm for the pneumatic system. The stiffness of the air spring model is expressed as a function of pressure, volume, area, and the polytropic index, but the process that determines the pressure of the air spring is not described. Nieto *et al.* (2008) derived a nonlinear model of an air spring on the basis of thermodynamics, assuming adiabatic or isothermal conditions, and analyzed the stiffness, the damping factor, and the transmissibility using the derived model. Chang and Lu (2008) also developed a model of an air spring on the basis of thermodynamics, which consisted of two steps. First, the air spring pressure is obtained using the adiabatic condition, and then it is corrected by considering the temperature obtained by the heat transfer equation. Because the model does not consider the air supply or the air exhaust to/from the air spring, it cannot be employed in the design of the pneumatic system or its control algorithm. In addition, it is difficult to employ the model for the stability analysis because the model is expressed by algebraic equations.

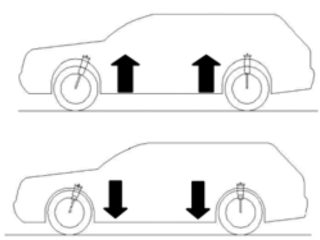

Figure 1. Adjustment of the height of a vehicle.

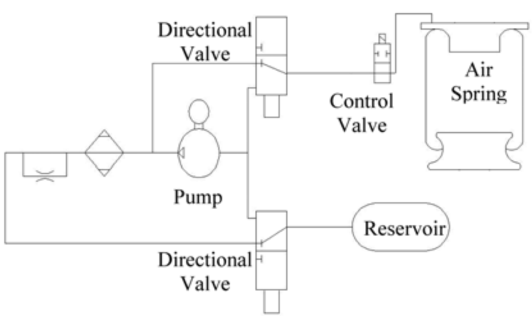

Figure 2. Air spring and its pneumatic supply system (Folchert, 2006; Jang *et al*., 2007).

The objective of this study is to develop the general air spring model on the basis of the thermodynamic equation without the assumption of adiabatic or isothermal conditions and with the variation of air mass. The analysis of the developed model will reveal the important factors that have a significant effect on the stiffness and hysteresis of an air spring. The author of this paper performed the study on the air spring model and its analysis in previous research (Cha *et al.*, 2006). The current study enhances the previous model of an air spring. The further analysis is performed on the basis of the enhanced model. Moreover, the stability of the air spring model is analyzed in this paper.

The rest of this paper is organized in the following order. In Section 2, the generalized model of the air spring is derived on the basis of the thermodynamic equation. In Section 3, the derived model is validated by experimental results, and the stability and important characteristics of the air spring such as the stiffness and hysteresis are analyzed. Finally, Section 4 presents a summary of the results and draws the conclusions.

2. MATHEMATICAL MODEL OF AIR SPRING

Figure 3 shows the control volume of the air spring, the main variables of which are pressure, absolute temperature, air mass and volume. The mathematical model of the air spring can be derived using the energy conservation law.

The flow of the air mass into or out of the control volume, shown in Figure 3, is controlled by the operation of the control valve in the pneumatic circuit, as shown in Figure 2. The flow of the air accompanies the enthalpy. In addition, work is performed on the control volume by the vehicle body and the wheel, and the difference of temper-

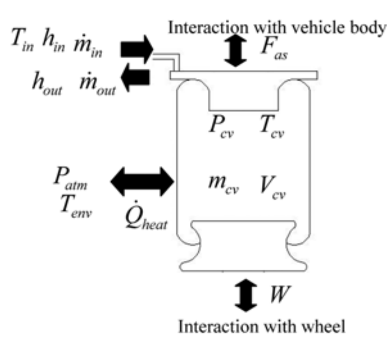

Figure 3. Control volume of the air spring.

atures between the inner and the outer sides of the control volume generates some heat transfer between them. These power flows can be modeled by the following energy conservation equation (Fernandez and Woods, 1999; Cha *et al*., 2006).

$$\dot{Q}_{heat}+\dot{W}+(h_{in}\dot{m}_{in}-h_{out}\dot{m}_{out})=\dot{U}_{cv} \tag{1}$$

where the time derivative of work that is performed on the control volume, $\dot{W}$, is defined using the pressure inside the control volume, P_{cv}, and the time derivative of the control volume, V_{cv}, by

$$\dot{W}=-P_{cv}\dot{V}_{cv} \tag{2}$$

The enthalpies flowing into and out of the control volume, h_{in} and h_{out}, are expressed using the specific heat at constant pressure, c_p, and the temperatures of the air mass flowing into and inside the control volume, T_{in} and T_{cv}, respectively, by

$$h_{in}=c_pT_{in}$$
$$h_{out}=c_pT_{cv} \tag{3}$$

The enthalpies multiplied by the air mass flow rate flowing into and out of the air spring, $\dot{m}_{in}$ and $\dot{m}_{out}$, represent power flows. The internal energy of the control volume, U_{cv}, is defined using the specific heat at constant volume, c_v, the air mass, m_{cv}, and the temperature inside the control volume by

$$U_{cv}=c_vm_{cv}T_{cv} \tag{4}$$

The heat transfer rate between the inner and the outer sides of the control volume, $\dot{Q}_{heat}$, is expressed using the heat transfer coefficient, h_c, the area of the heat transfer, A_{heat}, and temperatures of the outer and the inner sides of the control volume, T_{env} and T_{cv}, in the following form.

$$\dot{Q}_{heat}=h_cA_{heat}(T_{env}-T_{cv}) \tag{5}$$

To derive the pressure dynamic equation from the equation (1), the temperature inside the control volume is replaced with the pressure inside the control volume using the following ideal gas equation.

$$T_{cv}=\frac{1}{R}\frac{V_{cv}P_{cv}}{m_{cv}} \tag{6}$$

where R is the ideal gas constant. The derivative of the temperature inside the control volume with respect to time can be derived by differentiating equation (6) with respect to time, as follows:

$$\frac{\dot{T}_{cv}}{T_{cv}}=\frac{\dot{P}_{cv}}{P_{cv}}-\frac{\dot{m}_{cv}}{m_{cv}}+\frac{\dot{V}_{cv}}{V_{cv}} \tag{7}$$

where the air mass inside the control volume varies with the air mass flowing into and out of the control volume on the basis of the mass conservation law, as follows:

$$m_{cv}=\int\dot{m}_{cv}dt=\int(\dot{m}_{in}-\dot{m}_{out})dt \tag{8}$$

Finally, the first order differential equation for the pressure of the air in the control volume can be obtained from equations (1), (6), (7), the specific heat ratio $k=c_p/c_v$, and $R/c_v=k-1$ as follows:

$$\begin{aligned}\dot{P}_{cv}=&-kP_{cv}\frac{\dot{V}_{cv}}{V_{cv}}\\&+\frac{k-1}{V_{cv}}h_cA_{heat}\left(T_{env}-\frac{V_{cv}}{Rm_{cv}}P_{cv}\right)\\&+\frac{kR}{V_{cv}}\left(T_{in}\dot{m}_{in}-\frac{P_{cv}V_{cv}}{m_{cv}R}\dot{m}_{out}\right)\end{aligned} \tag{9}$$

Equation (9), which represents the mathematical model for the air spring, consists of two kinds of variables, in which the specific heat ratio, heat transfer coefficient, and the area of heat transfer are the parameters, and the volume and the rate of change of the volume in the air spring, the air mass flow rates, and the temperature of the environment are the variables determined by the components connected to the air spring. Each parameter was obtained through the following methods. The ideal gas constant was selected from the property of the air, and the air mass inside the air spring was calculated from the ideal gas equation. The specific heat ratio was estimated from the comparison between the experimental and simulation results. The area of heat transfer and the volume of the air spring were calculated from the measured geometric data and adjusted through the comparison between the experimental and simulation results. The heat transfer coefficient was selected from the well-known heat transfer coefficients and adjusted through the comparison between the experimental and simulation results.

Equation (9) can be transformed into the following state space form.

$$\dot{P}_{cv}=a(t)P_{cv}+u(t) \tag{10}$$

where t stands for time, and $a(t)$ and $u(t)$ represent functions of time defined by

$$a(t)=-k\frac{\dot{V}_{cv}}{V_{cv}}-\frac{(k-1)h_cA_{heat}}{R}\frac{1}{m_{cv}}-k\frac{\dot{m}_{out}}{m_{cv}} \tag{11}$$

$$u(t)=(k-1)h_cA_{heat}\frac{T_{env}}{T_{cv}}+kR\frac{T_{in}\dot{m}_{in}}{V_{cv}} \tag{12}$$

This representation is used for the stability analysis of the dynamic equation. Although this equation is a first order

Table 1. Parameters for the air spring model.

R	287 J/kgK
T_{env}	293.15 K
m_{cv}	0.012 kg
A_{heat}	0.050 m^2 (at maximum)
k	1.17~1.3 (for 0.05~5 Hz)

linear system, its stability cannot be determined by only the sign of the time constant, $a(t)$, because the dynamic equation (10) is not a time invariant system. The stability for the dynamic system will be analyzed in the next section.

The pressure inside the air spring, which is determined by equation (10), is transformed into the force acting on the vehicle body

$$F_{as}=A_{eff}(P_{cv}-P_{atm}) \tag{13}$$

where F_{as} is the force, A_{eff} is the effective area of the air spring, through which pressure is transformed into the force, and P_{atm} is the pressure of the environment.

3. ANALYSIS AND VALIDATION OF AIR SPRING MODEL

The air spring model of equation (9) was developed to describe the important characteristics such as the hysteresis and nonlinear spring stiffness. The experimental results for the air spring validate the mathematical model, and the factors that affect the stiffness and the hysteresis of the air spring are analyzed in this section.

3.1. Experiments of the Air Spring

Figure 4 briefly shows the experimental setup where a sinusoidal displacement is vertically applied to the air spring by a linear actuator, which is positioned in the lower part of the air spring instead of the road excitation. The force, which is applied to the vehicle body by the air spring, is measured by the sensor which is positioned in the upper part of the air spring. The pressure of the air spring is measured by the sensor, which is positioned in the air passage between the air spring and the control valve. Experiments in which the air spring is excited at various frequencies are performed. Through the experiments, the signals such as vertical displacement which represents the vertical movement of the wheel with respect to the vehicle body, the pressure inside the air spring and the force are measured to validate the established model.

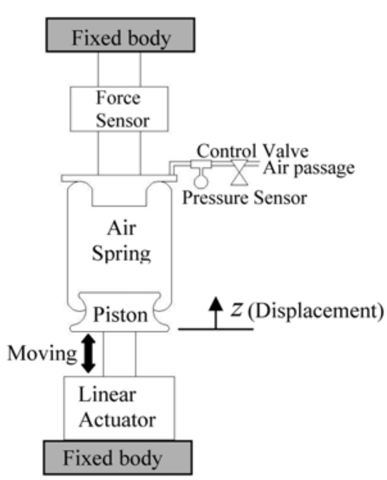

Figure 4. Schematic representation of the experimental setup.

Table 2. Experimental conditions.

Initial pressure	7.7 bar (absolute pressure)
Environment temperature	Room temperature
Displacement input (sinusoid)	10 mm (amplitude) 0.05 Hz, 0.5 Hz, 5 Hz (frequency)

3.2. Analysis and Validation for Hysteresis

The experimental data on the forces generated by the air spring are plotted versus the vertical displacement in Figure 5, which clearly shows the hysteresis. Because the force is

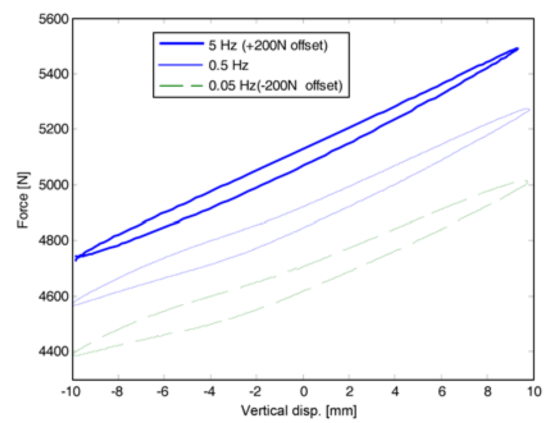

Figure 5. Experimental results of force versus vertical displacement for sinusoidal motion excitation at 0.05 Hz, 0.5 Hz and 5 Hz (the 0.05 Hz and 5 Hz data are represented 200 N lower and higher than the actual values for ease in distinction between the different data plots, respectively).

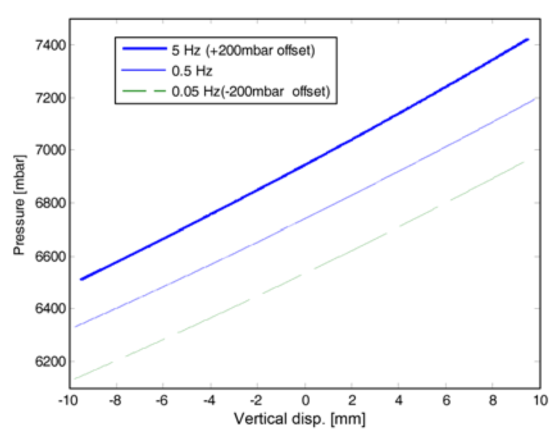

Figure 6. Simulation results for pressure response due to only variation of the volume for sinusoidal motion excitation at 0.05 Hz, 0.5 Hz and 5 Hz (the 0.05 Hz and 5 Hz data are represented 200 mbar lower and higher than the actual values, respectively).

the effective area times the pressure, the cause of the hysteresis can be found in the pressure dynamic equation (9). The inspection of equation (9) reveals that the hysteresis can be caused by three terms.

The first term, $-kP_{cv}\dot{V}_{cv}/V_{cv}$, occurs due to the volume change in an air spring according to the vertical displacement. The hysteresis on the pressure response can occur when the volume is a function of other variables as well as the vertical displacement. However, for the fixed air mass and the given temperature, the volume of the air spring is assumed to be a function of only the vertical displacement on the basis of test results on some air springs. Hence, the pressure responses due to only the variation of the volume, which is a function of only the vertical displacement, do not show the hysteresis as in Figure 6.

The second term, $\frac{k-1}{V_{cv}}h_c A_{heat}\left(T_{env}-\frac{V_{cv}}{Rm_{cv}}P_{cv}\right)$, which occurs due to the heat transfer between the air spring and the environment, is a function of the pressure as well as the vertical displacement. The hysteresis due to this second term can be analyzed through the pressure dynamic equation, which consists of the first term and the second term as follows:

$$\begin{aligned}\dot{P}_{cv}&=a(t)P_{cv}+u(t)\\ a(t)&=-k\frac{\dot{V}_{cv}}{V_{cv}}-\frac{(k-1)h_c A_{heat}}{Rm_{cv}}\\ u(t)&=(k-1)h_c A_{heat}\frac{T_{env}}{V_{cv}}\end{aligned}\tag{14}$$

This equation has the form of a first-order low-pass filter in which $a(t)$ is the cut-off frequency, $u(t)$ is the input signal, and P_{cv} is the filtered output signal. The low-pass filter causes the phase shift of the output signal with respect to the input signal, which in turn generates the hysteresis of the output signal with respect to the input signal. Because $a(t)$ is time-varying, equation (14) represents the characteristics that are significantly different from the low-pass filter with a time-invariant cut-off frequency. However, the first order dynamics of equation (14) generate the phase shift between the input and the output, which causes the hysteresis in the pressure output. More specifically, the phase shift of the pressure output with respect to the displacement input decreases as the frequency of the input increases from 0.05 Hz to 5 Hz, which decreases the magnitude of the hysteresis in the pressure, as shown in Figure 7. (Pressures of all the figures in this paper represent the relative pressure.) In addition, the variation of the magnitude of the hysteresis can also be shown in the following equation, which is derived by considering only the first term and the second term of equation (9) when the sinusoidal vertical displacement, $z=z_0\sin(2\pi f t)$, is applied to the air spring.

$$\frac{dP_{cv}}{dz}=-\frac{kP_{cv}}{V_{cv}}\frac{dV_{cv}}{dz}+\frac{(k-1)h_c A_{heat}}{2\pi f z_0\cos(2\pi f t)V_{cv}}\left(T_{env}-\frac{V_{cv}}{Rm_{cv}}P_{cv}\right)\tag{15}$$

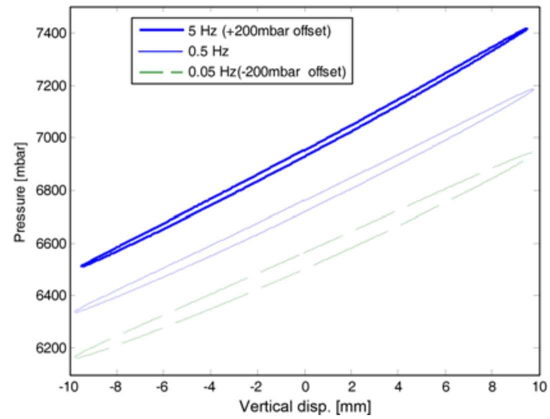

Figure 7. Simulation results of pressure versus vertical displacement for sinusoidal motion excitation at 0.05 Hz, 0.5 Hz and 5 Hz (the 0.05 Hz and 5 Hz data are represented 200 mbar lower and higher than the actual values, respectively).

where z_0 and f represent the magnitude and the frequency of the vertical displacement sinusoid, respectively. This equation indicates that the increase of the frequency reduces the effect of the hysteresis due to the second term.

The simulated pressure responses shown in Figure 7 are compared with the experimental results shown in Figure 8, which are obtained without the air mass flowing into or out of the air spring. The similarity between the simulation and experimental results validates the air spring model developed and its analysis.

The third term, $\frac{kR}{V_{cv}}\left(T_{in}\dot{m}_{in}-\frac{P_{cv}V_{cv}}{m_{cv}R}\dot{m}_{out}\right)$, in equation (9) occurs when air is supplied to or exhausted from the air spring, which means that the vehicle body is lifted or lowered for some specific purpose, as shown in Figure 1.

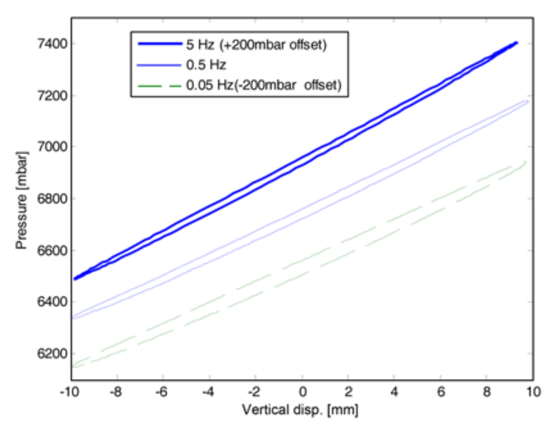

Figure 8. Experimental results of pressure versus vertical displacement for sinusoidal motion excitation at 0.05 Hz, 0.5 Hz and 5 Hz (the 0.05 Hz and 5 Hz data are represented 200 mbar lower and higher than the actual values, respectively).

This term is also a function of the pressure as well as the vertical displacement and is expressed including the first term by the first order filter form as follows:

$$\dot{P}_{cv}=\left(-k\frac{\dot{V}_{cv}}{V_{cv}}-k\frac{\dot{m}_{out}}{m_{cv}}\right)P_{cv}+kR\frac{T_{in}\dot{m}_{in}}{V_{cv}} \tag{16}$$

Unlike the second term, the third term does not show the typical form of a hysteresis but shows the pressure responses presented in Figure 9. This figure represents the pressure responses due to the first term and the third term when the upper part of the air spring is lowered by 10 mm, which means that the vehicle height is lowered when the lower part of the air spring is excited at 0.5 Hz. In Figure 9, the thin lines represent the pressure responses before and after the variation of the air mass inside the air spring, and the thick line stands for the pressure response while the air mass varies. This figure indicates that the variation of the

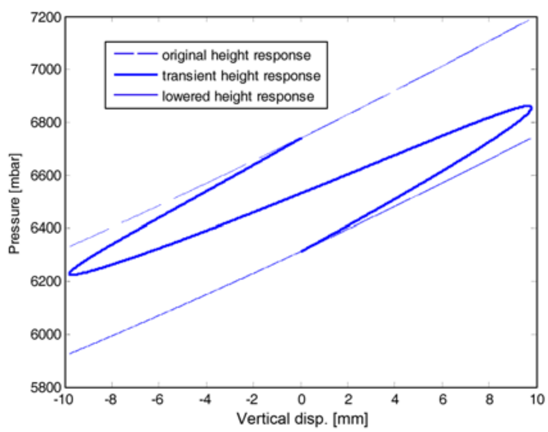

Figure 9. Simulation results for pressure responses due to the variations of the volume and the air mass inside the air spring.

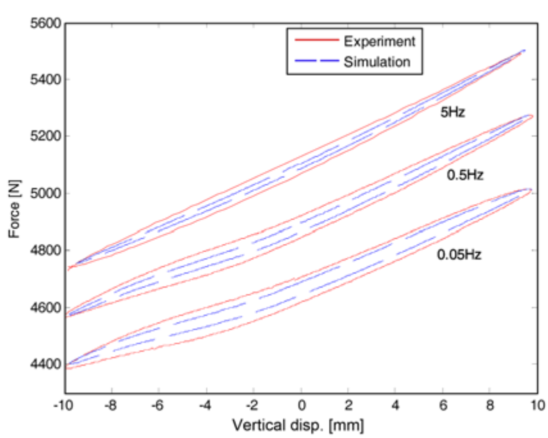

Figure 10. Force responses for sinusoidal motion excitation at 0.05 Hz, 0.5 Hz and 5 Hz (the 0.05 Hz and 5 Hz data are represented 200 N lower and higher than the actual values, respectively). Simulation results do not include the hysteresis of the effective area while experimental results include it.

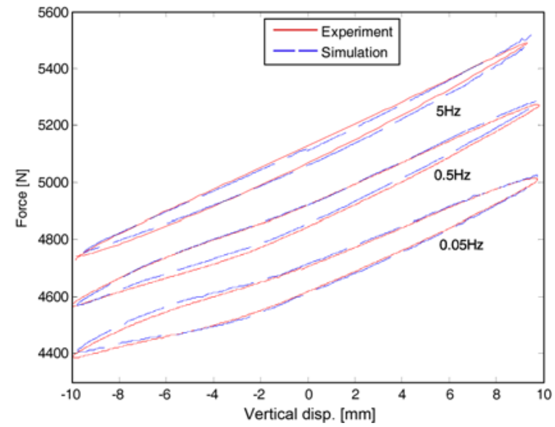

Figure 11. Force response for sinusoidal motion excitation at 0.05 Hz, 0.5 Hz and 5 Hz (the 0.05 Hz and 5 Hz data are represented 200 N lower and higher than the actual values, respectively). Simulation results include all effects except the air mass variation.

air mass inside the air spring has an effect on the pressure response, but no hysteresis occurs due to the variation of the air mass.

Because the force is defined by the effective area times the pressure such as expressed in equation (13), the effective area in addition to the pressure has an effect on the hysteresis of the force response. The effective area varies with the vertical displacement because it varies with the vertical shape of the contour of the piston in the lower part of the air spring, which changes the ride comfort of the vehicle. In addition, the effective area varies with the pressure at the same displacement, which yields the hysteresis of the effective area. In Figures 10 and 11, the effect of this hysteresis is represented. Simulation results in Figure 10 do not include the hysteresis of the effective area, while those in Figure 11 include it. These figures show that the hysteresis of the effective area enlarges the hysteresis of the force response. Finally, the comparison between the simulated and the experimental results in Figure 11 confirms the validity of the air spring model.

3.3. Analysis and Validation of Stiffness

The stiffness of the air spring can be obtained by differentiating equation (13) with respect to the vertical displacement, as follows:

$$k_{as}=\frac{dF_{as}}{dz}=A_{eff}\frac{dP_{cv}}{dz}+(P_{cv}-P_{atm})\frac{dA_{eff}}{dz} \tag{17}$$

where k_{as} represents the stiffness of the air spring, and z the vertical displacement. This equation indicates that the stiffness of the air spring varies with the derivatives of the pressure and the effective area with respect to the vertical displacement.

In equation (9), the first term, which represents the effect of the volume variation, is one of the factors that change the stiffness of the air spring expressed in equation (17). The variation of the pressure due to the first term is rewritten in the following equation.

$$\frac{dP_{cv}}{dz}=-kP_{cv}\frac{1}{V_{cv}}\frac{dV_{cv}}{dz} \tag{18}$$

$$=kP_{cv}\frac{A_{cs}}{V_{cv0}+\int_{curr}^{z_{\max}}A_{cs}dz} \tag{19}$$

where V_{cv0} stands for the fixed volume like the additional volume attached to some air spring in order to improve the comfort, A_{cs} represents the cross-sectional area of the air spring, and $z_{\max}$ and z_{curr} are the maximum displacement and the current displacement of the bottom of the air spring, respectively. It is well known that an increase of the volume of the air spring reduces the stiffness of the air spring. However, a close inspection of equation (18) reveals that the absolute value of the derivative of the pressure with respect to the vertical displacement, which represents a part of the stiffness expressed in equation (17), decreases as the entire volume of the air spring increases but increases as the derivative of the volume with respect to the vertical displacement increases. Hence, the derivative of the pressure increases, which increases the stiffness, if the increment of the derivative of the volume is larger than the increment of the volume even though the entire volume increases. The term, $V_{cv0}+\int_{curr}^{z_{\max}}A_{cs}dz$, in the denominator of equation (19) represents the entire volume, and the cross-sectional area, A_{cs}, in the numerator stands for the derivative of the entire volume with respect to the vertical displacement. When the cross-sectional area increases, the increment of the derivative of the volume is larger than the increment of the entire volume. For example, when the cross-sectional area increases by 50 percent, the entire volume cannot increase by up to 50 percent because the fixed volume does not increase. Hence, the increase of the volume due to the cross-sectional area increases the stiffness of the air spring, while the increase of the volume without the variation of the cross-sectional area decreases the stiffness.

The heat transfer, which is included in the second term of equation (9), also has an effect on the variation of the stiffness. Equation (15) clearly shows the variation of the stiffness due to the heat transfer. In equation (15), the derivative of the pressure with respect to the displacement due to the heat transfer is added to that due to the variation of the volume, which changes the stiffness due to the variation of the volume. In addition, because the term due to the heat transfer is divided by the frequency of the displacement in equation (15), the stiffness due to the heat transfer is reduced as the frequency increases. The stiffness variation with frequency is shown in Figure 12, which represents the pressure responses due to only the heat transfer. The entire pressure response in equation (15) is determined by the sum of Figure 6 and Figure 12. Hence, the heat transfer at the low frequency has a significant effect on the entire stiffness, unlike that at the high frequency. More specifically, the heat transfer at the low frequency significantly reduces the stiffness due to the variation of the volume, while at the high frequency it slightly reduces the stiffness. The negative pressure in Figure 12 occurs for the following reason. When the air spring is compressed, the pressure increases due to the compressed volume. The resulting increment of the pressure increases the temperature of the air spring in equation (6) and decreases the rate of change of pressure due to the second term in equation (15). Consequently, when the temperature of the air spring becomes larger than that of the environment, the pressure due to heat transfer decreases, which can yield a negative pressure. However, the entire pressure increases because the increase of the pressure due to the volume variation is larger than the decrease of the pressure due to the heat transfer even when the temperature of the air spring is larger than the environment.

The pressure response due to the variation of the air mass, which is included in the third term of equation (9), is also added to that due to the other two terms, which in turn changes the stiffness which is determined by the other terms. The equation (9) shows that the mass flow rate flowing into the air spring, $\dot{m}_{in}$, increases the stiffness, while the mass flow rate flowing out of the air spring, $\dot{m}_{out}$, decreases it. Figure 9 represents the pressure response due to variations of the volume and the air mass when the air mass is flowing out of the air spring.

In addition to the pressure variation, the variation of the effective area has an effect on the stiffness. As mentioned earlier, the contour of the piston of the air spring is manufactured in order to obtain the optimum ride comfort, which yields the variation of the effective area. Hence, the large variation of the effective area can have a significant effect on the variation of the stiffness. This study on the air spring which was employed in this experiment shows that most of values of the stiffness due to the second term in equation (17), which represents the effect of the effective area variation, vary within 40% of the entire stiffness.

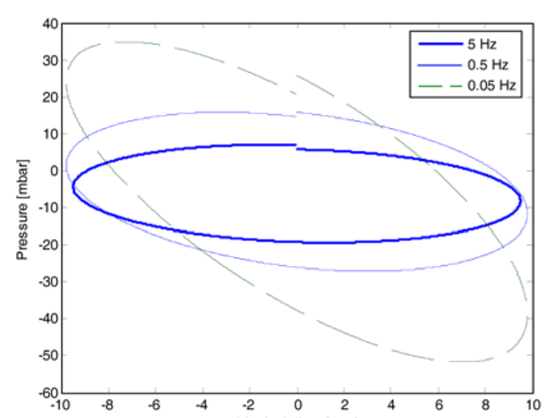

Figure 12. Simulation results for pressure response due to only heat transfer for sinusoidal motion excitation at 0.05 Hz, 0.5 Hz and 5 Hz.

The slopes of the force curves in Figure 11 represent the entire stiffness, which includes the rate of change of the effective area as well as the pressure. Figure 11 indicates that the stiffness varies with the displacement and frequency. In addition, it is observed that the stiffness of the simulation curves is similar to that of experimental curves in the full range of the displacement.

3.4. Stability Analysis of the Air Spring System

The stability of the air spring is very important for the vehicle stability. However, the stability of the pressure dynamics of the air spring is not simply determined like a time-invariant system because $a(t)$ in the air spring model equation (10) is time-varying.

For the stability analysis of the dynamic equation (10), linear time-invariant dynamic systems are introduced as follows:

$$\dot{P}_{max}=a_{max}P_{max}+u(t)$$
$$\dot{P}_{min}=a_{min}P_{min}+u(t) \tag{20}$$

where P_{max} and P_{min} are the pressure variables, and a_{max} and a_{min} are the constant maximum and minimum values of $a(t)$. Because $a(t)$ is bounded by a_{max} and a_{min}, P_{cv} is also bounded by P_{max} and P_{min} as follows:

$$\dot{P}_{min}\leq\dot{P}_{cv}\leq\dot{P}_{max} \tag{21}$$

Because equation (20) is a linear time-invariant system, P_{max} and P_{min} are bounded if a_{max} and a_{min} are negative values and the input, $u(t)$, is bounded (Khalil, 1996). $u(t)$ in the equation (12) is bounded when the air mass flow rate flowing into the air spring, $\dot{m}_{in}$, is bounded. Consequently, the pressure of the air spring, P_{cv}, is bounded, when $\dot{m}_{in}$ is bounded and the following condition is satisfied.

$$a(t)=-\left(k\frac{\dot{V}_{cv}}{V_{cv}}+\frac{(k-1)h_cA_{heat}}{Rm_{cv}}+k\frac{\dot{m}_{out}}{m_{cv}}\right)<0 \tag{22}$$

This stability criterion is a sufficient condition because it has not been proven that the air spring model is unstable if the derived stability condition is not satisfied.

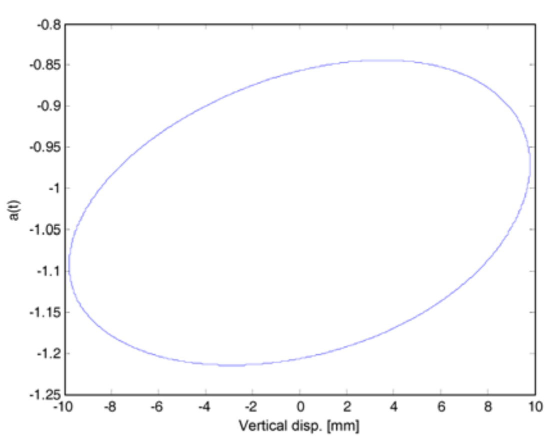

Figure 13. Values of the variable, $a(t)$, of equation (22) for sinusoidal motion excitation at 0.5 Hz when there is no air mass flowing into or out of the air spring.

Equation (22) indicates that the increase of the fixed volume of the air spring, the heat transfer coefficient and area, and the air mass flow rate flowing out of the air spring are helpful in satisfying the stability condition (22), while the increase of the negative rate of change of the volume and the air mass prevent the stability condition (22) from being satisfied. Figure 13 shows that $a(t)$ has the negative values for sinusoidal motion excitation at 0.5 Hz. For other sinusoidal motion excitation of 0.05 Hz and 5 Hz, $a(t)$ also has the negative value.

4. CONCLUSION

This research developed a general model of an air spring based on thermodynamics. This model was derived from the energy conservation law. The thermodynamic parameters inside the air spring are assumed to be uniform, which means that the parameters do not vary with the position inside the air spring. The air inside an air spring is also assumed to have an ideal gas property, and the kinetic and potential energies of the air are neglected. However, the resulting model can represent all processes ranging from isothermal to adiabatic conditions because the assumption that the process is adiabatic or isothermal has not been employed. In addition, the model can be used to simulate the system with the pneumatic circuit able to adjust the vehicle height because it includes the air mass flowing into and out of the air spring.

The analysis of the established model revealed that the volume variation, the heat transfer, the variation of the air mass and the effective area have an effect on the stiffness and hysteresis. The heat transfer yields the larger hysteresis under the input with the low frequency than that with the high frequency, and the effective area enlarges the hysteresis. In addition, the heat transfer significantly reduces the stiffness at the low frequency, and the air mass flow rate flowing into the air spring increases the stiffness, while the air mass flow rate flowing out of the air spring decreases it. In particular, the increase of the volume due to the cross-sectional area increases the stiffness, while the increase of the volume due to the other reason decreases it. Additionally, most of the stiffness due to the effective area varied within about 40% of the entire stiffness for the air spring used in this study.

The stability condition for the air spring was also derived from the study regarding the established time-varying model. The inspection of the stability condition revealed that the increases of the fixed volume, the heat transfer coefficient and area as well as the air mass flow rate flowing out of the air spring have a positive effect on the stability, while the increases of the negative rate of change of the volume and the air mass have a negative effect on it. However, the analysis for the parameters has some limitation because the derived stability criterion is a sufficient condition.

Simulation results of the model were presented, and these were in substantial agreement with experimental measurements of force and pressure with respect to displacement excitations of 0.05 Hz, 0.5 Hz, and 5 Hz, which validates the modeling approach presented here for the air spring. The resulting validated model will be especially useful for the study of air spring systems including the pneumatic circuit and its control algorithm.

REFERENCES

Cha, C. J., Kim, P. G. and Lee, S. J. (2006). Development of an analytical air spring model with hysteresis characteristics. *Fall Conf. Proc., Korean Society of Automotive Engineers*, 1964−1969.

Chang, F. and Lu, Z.-H. (2008). Dynamic model of an air spring and integration into a vehicle dynamics model. *Proc. Institution of Mechanical Engineers, Part D, J. Automobile Engineering* **222**, **10**, 1813−1826.

Fernandez, R. and Woods, R. L. (1999). Thermal considerations in fluid power systems modeling. *Proc. Fluid Power Systems and Technology*, 47−54.

Folchert, U. (2006). *Air Supply System for a Motor Vehicle*. Continental Aktiengesellschaft US Patent No. 7097166.

Hyundai Motor Company (2009). *Instruction Manual for GENESIS*. 5−35.

Jang, I., Kim, H., Lee, H. and Han, S. (2007). Height control and failsafe algorithm for closed loop air suspension control system. *Proc. Int. Conf. Control, Automation and Systems*, 373−378.

Khalil, H. K. (1996). *Nonlinear Systems.* 2nd Edn. Prentice Hall. New Jersey.

Kia Motor Company (2009). *Instruction Manual for MOHAVE,* **5**, 37−38.

Kim, W., Lee, J. W., Kim, H. K., Doo, M. S., Kim, H. S. and Doh, W. J. (2001). Handling analysis of active height control system for SUV using ADASMS. *Fall Conf. Proc., Korean Society of Automotive Engineers*, 908–914.

Kim, W. Y. and Kim, D. K. (2005). Improvement of ride and handling characteristics using multi-objective optimization techniques. *Int. J. Automotive Technology* **6**, **2**, 141−148.

Nieto, A. J., Morales, A. L., Gonzalez, A., Chicharro, J. M. and Pintado, P. (2008). An analytical model of pneumatic suspensions based on an experimental characterization. *J. Sound and Vibration* **313**, **1/2**, 290–307.

Quaglia, G. and Sorli, M. (2001). Air suspension dimensionless analysis and design procedure. *Vehicle System Dynamics* **35**, **6**, 443−475.

Seong, J. H., Lee, K. W., Park, G. B. and Yang, H. J. (2008). Study on air spring modeling method for railway vehicle dynamics. *Proc. Spring Conf., Korean Society for Railway*, 2216–2221.